Measurement of earplugs insertion loss using a classical impedance tube

Olivier Doutres[a)]
Department of Mechanical Engineering, École de technologie supérieure, 1100 rue Notre-Dame Ouest, Montréal, Québec H3C 1K3, Canada

Franck Sgard [b)]
IRSST, Direction Scientifique, 505 Boulevard de Maisonneuve Ouest, Montréal, Québec H3A 3C2, Canada

Guilhem Viallet[c)]
Department of Mechanical Engineering, École de technologie supérieure, 1100 rue Notre-Dame Ouest, Montréal, Québec H3C 1K3, Canada

This work presents a new method for assessing the normal incidence insertion loss (IL) of earplug (EP) by the use of a classical impedance tube. The proposed technique allows for fast and straightforward IL measurements and thus is particularly suitable for earplug testing in a design phase. Indeed, compared to standard ATF measurements, the proposed method does not require cumbersome experimental facilities (i.e., reverberant or anechoic chambers). In the proposed method, the EP (≈ 10 mm outer diameter) is inserted in a rigid sample holder which is itself placed in a larger diameter impedance tube (commonly 29 mm inner diameter). The transfer matrix of the system is measured according to a standardized procedure. The transfer matrix of the EP alone is then recalculated by eliminating the effect of the sample holder. Finally, the IL is estimated by coupling the EP transfer matrix to a one-dimensional model of the occluded ear canal taking into account for the tympanic membrane. The proposed method is tested numerically using a two-dimensional acoustical finite element model (FEM) of a cylindrical impedance tube and is validated by comparison with IL simulations computed from another numerical model of an occluded ear canal.

[a)] email: olivier.doutres@etsmtl.ca
[b)] email: franck.sgard@irsst.qc.ca
[c)] email : guilhemviallet@etsmtl.ca

1 INTRODUCTION

Objective measurement of EP insertion loss is commonly performed by the use of an acoustical test fixture (ATF). This fixture consists of a synthetic human outer ear inserted in artificial head and torso. The most sophisticated ATF available in the market accounts for (1) the eardrum impedance by the use of a dedicated coupler, (2) the ear canal skin tissue by the use of a silicone layer and (3) the human body temperature in the ear from heaters. Such objective measurement setup allows for quick and repeatable measurements and is particularly suitable for quality control, earplug design and experiments in high noise level environments[1]. However, ATF suffers of three main disadvantages: (1) ATF measurements are not always representative of the real earplug performance since all the human head features and human factors (e.g., quality of EP insertion, comfort…) are not taken into account[1], (2) cumbersome and expensive experimental facilities (e.g., reverberant or anechoic chambers) are required in order to apply a controlled acoustic field on the ATF and (3) the ear canal geometry and coupler included in the ATF have been designed to replicate the average acoustical properties of normal adult ears but it is very unlikely that these averaged properties actually correspond to any real person[2]. In an attempt to better understand the intrinsic properties of EPs, Hiselius[3,4] proposed another objective method based on the use of a small impedance tube (9 mm inner diameter). The EPs are described as Two-ports and their acoustics properties are measured from sound pressure levels carried out on both sides of the EP for two different impedance tube terminations. The *IL* of EPs is finally assessed by numerically coupling the Two-port of the EP and that on an ear. Unlike ATF, this method allows one to compute the *IL* for various ear canal geometries and tympanic membrane impedances. Another advantage related to this technique is the ease of generation and control of the excitation sound field within the impedance tube. This paper proposes a very similar approach for assessing the objective insertion loss of earplugs: i.e., the EP acoustic properties are measured separately by the use of an impedance tube and coupled to a model of the ear in order to estimate the *IL*. This work can thus be seen as an extension of Hiselius' work and the main improvements are listed below: (1) the earplug acoustic properties (i.e., reflection coefficient, sound transmission loss coefficient) are measured in an impedance tube following a standard procedure[5], (2) the proposed method allows for measuring the EP acoustic properties in large impedance tube commonly available in the market (29 mm inner diameter), which avoids several technical difficulties experienced in refs. [3,4], (3) the sample holder can mimic the ear canal geometry and includes the soft tissues, (4) the analytical model used to compute the *IL* from earplug acoustic properties is based on the wavefield decomposition theory, which leads to straightforward analytical relations between EP and ear canal acoustics properties.

This paper is organized as follows. In section 2, the analytical model of the open and occluded ear is presented. An analytical relation between the EP insertion loss, two EP acoustic properties and ear canal acoustic properties is provided. This section also briefly describes the standard method for measuring the EP acoustic properties. The proposed impedance tube experimental procedure for assessing the *IL* is validated from numerical simulations. Section 3 presents the two main numerical models. The first model mimics the impedance tube measurements of the EP acoustic properties. The *IL* is then computed by coupling the simulated EP acoustic properties to a one-dimensional model of the occluded ear. The second numerical model simulates the artificial ear of an ATF (ATF 45CB, G.R.A.S. Sound & Vibration AS, Denmark). The associated *IL*, considered as reference, is computed from the sound pressure level at the tympanic membrane in the case of the open and occluded ATF ear canal. Section 4

presents the main results and discusses the impact of the sample holder used during the impedance tube simulations.

2 THEORY

2.1 Analytical model of the open and occluded ear canal

A schematic view of the open and occluded ear canal is shown in Fig. 1(a) and 1(b) respectively. The ear canal (EC) of total length l_{EC} is connected to the surrounding air at $x = 0$ and to the tympanic membrane (TM) at $x = l_{EC}$. In Fig. 1(b) the EC is occluded by an ear plug of thickness L. The EP is fully inserted in Fig. 1 but the proposed method can also be applied to other insertion depths. The acoustic pressure field is calculated in two acoustic domains: the entire EC in the case of the open ear (referred to as domain A in Fig. 1(a)) and the air cavity between the rear face of the EP and the TM in the case of the occluded EC (referred to as domain B in Fig. 1(b)). The acoustic pressure field within these two domains is described using the wavefield decomposition theory. These complex wavefields are decomposed in terms of forward and backwards propagating plane waves. The entrance of the EC is supposed to be flush mounted onto a rigid baffle. The pressure generated at the EC entrance by an incoming normal incident plane wave is twice the amplitude of the incident pressure P_0. In the case of the open ear canal (see Fig. 1(a)), the radiation impedance Z_r at the EC entrance is taken into account and approximated as the one of a baffled circular piston. At the opposite end of the EC, the TM is taken into account as a locally reacting impedance Z_{TM}. The lumped model corresponding to the coupler IEC711 is used as documented in reference[6]. On both sides of the EC, the boundary conditions are rather described in this work considering reflection coefficients r_r and r_{TM} in place of acoustic impedances Z_r and Z_{TM}, respectively.

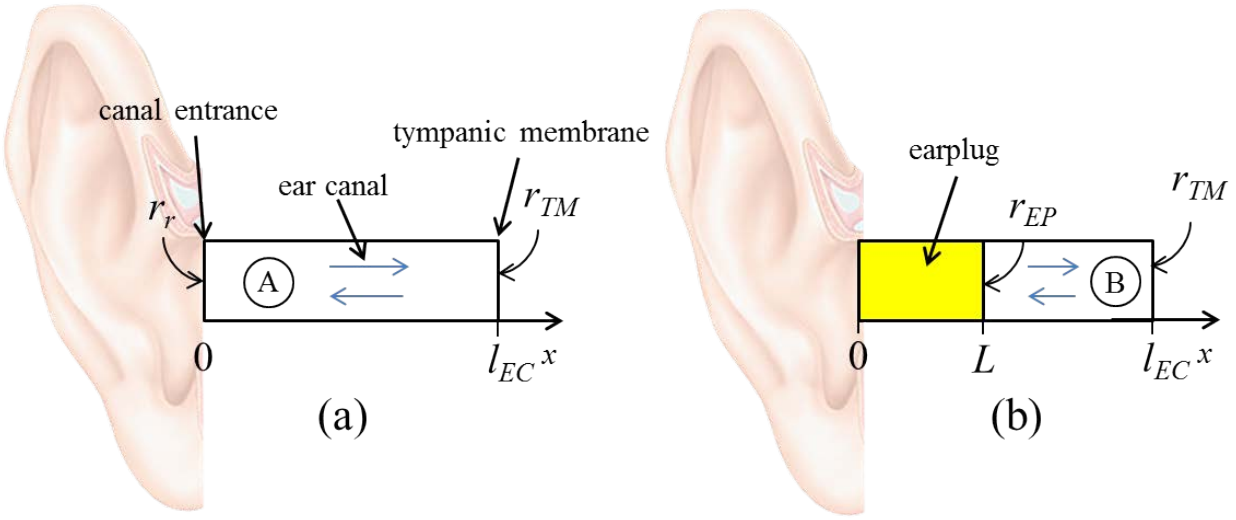

Fig. 1 – Schematic representation of the (a)open ear canal and (b) occluded ear canal.

Taking into account for the multiple wave reflections in domains A (open EC) and B (occluded EC), the total sound pressure fields at a position *x* within each of the domain are given respectively by:

$$p_{open}(x) = \frac{2P_0\left(e^{-jk_0x} + r_{TM}e^{-2jk_0l_{EC}}e^{jk_0x}\right)}{1 - r_r r_{TM}e^{-2jk_0l_{EC}}}, \quad \text{for} \quad 0 \le x \le l_{EC} \tag{1}$$

and

$$p_{occluded}(x) = \frac{P_0\tau_{EP}\left(e^{-jk_0x} + r_{TM}e^{-2jk_0l_{EC}}e^{jk_0x}\right)}{1 - r_{EP}r_{TM}e^{-2jk_0(l_{EC}-L)}}, \quad \text{for} \quad L \le x \le l_{EC}. \tag{2}$$

Here, k_0 is the wave number in the ambient fluid. r_{EP} is the EP reflection coefficient seen by the *x*-negative propagating waves in the acoustic domain B. It is thus the reflection coefficient of the EP backed by an infinite air layer. τ_{EP} is the sound transmission coefficient of the EP. It is defined as the fraction of airborne sound power incident on the EP that is transmitted by the EP and radiated on the other side. The insertion loss of the EP is obtained from the following expression

$$IL = L_{p,open} - L_{p,occluded}, \tag{3}$$

where L_p denotes the sound pressure level calculated in both cases at the tympanic membrane $x = l_{EC}$. According to Equations (1) and (2), the *IL* can thus be written as:

$$IL = TL_{EP} + IL_c, \tag{4}$$

with:

$$TL_{EP} = 20\log_{10}\left(\frac{1}{|\tau_{EP}|}\right), \tag{5}$$

and

$$IL_c = 20\log_{10}\left(\frac{2\left|1 - r_{EP}r_{TM}e^{-2jk_0(l_{EC}-L)}\right|}{\left|1 - r_r r_{TM}e^{-2jk_0l_{EC}}\right|}\right). \tag{6}$$

Equations (4)-(6) show explicitly that the EP insertion loss depends on the EP attenuation efficiency (from TL_{EP}) and on the sound absorption properties within the acoustic domain B (through the reflection coefficients r_{EP} and r_{TM}). These equations also indicate that *IL* can be estimated experimentally from the measurements of two EP acoustic properties: the transmission loss TL_{EP} and the reflection coefficient r_{EP} (see section 2.2 for their determination). These two properties are independent of (1) the occluded EC geometry (i.e, the length of the air cavity between the rear face of the EP and the TM related to the insertion depth) and (2) the acoustic boundary conditions upstream and downstream the EP (i.e., the acoustic impedance of the TM and the radiation impedance of the open ear). The impact of these acoustic boundary conditions is included afterward using Equation (6). Furthermore, the effect of lateral earplug boundary conditions (e.g, presence of skin, ear canal

geometry…) are implicitly accounted for during the determination of the earplug properties TL_{EP} and r_{EP}.

The proposed analytical approach is valid only if plane waves propagate inside the EC. This assumption is acceptable in the frequency range of interest (f<5 kHz) since the first transverse acoustic mode of an EC having an average diameter of around 7.5 mm (see ref.[7], page 284) is expected to occur above 20 kHz. The upper frequency limit decreases to 6 kHz if one uses a 29 mm impedance tube for measuring the EP acoustic properties. Viscous and thermal dissipations within the ear canal (acoustic domains A and B) are not modeled here given the diameter of the EC and the considered frequency range. However, one can account for these effects using a complex and frequency dependent wavenumber k_0 based on effective properties of the air in the EC calculated from a cylindrical pore model[8].

Even if this work focuses on the *IL*, the same modelling approach can be used to derive a straightforward analytical relation between the EP insertion loss and the noise reduction coefficient *NR*. *NR* is calculated from the difference of the sound pressure level estimated at the entrance of the EC ($x=0$) and inside the occluded acoustic domain B: $NR = L_{p,x=0} - L_{p,L\le x\le l_{EC}}$. Depending on the position x inside the domain B ($L \le x \le l_{EC}$) used to estimate the *NR*, the relation writes:

$$NR(x) = IL - 20\log_{10}\left(\frac{\left|e^{-jk_0x} + r_{TM}e^{-2jk_0l_{EC}}e^{jk_0x}\right|}{\left|1 - r_r r_{TM}e^{-2jk_0l_{EC}}\right|}\right). \tag{7}$$

In the particular case where *NR* is calculated at the tympanic membrane ($x = l_{EC}$), Equation (7) can be rewritten as

$$NR(l_{EC}) = IL - TFOE, \tag{8}$$

with *TFOE* the transfer function of the open ear given by

$$TFOE = 20\log_{10}\left(\frac{\left|1 + r_{TM}\right|}{\left|1 - r_r r_{TM}e^{-2jk_0l_{EC}}\right|}\right). \tag{9}$$

2.2 Earplug acoustic properties

The two EP acoustic properties (TL_{EP} and r_{EP}) are measured under normal incidence plane waves in an impedance tube according to the standard ASTM E2611-09[5]. Since the standard is based on the transfer matrix method (TMM), the EP is represented by a 2×2 transfer matrix T^{EP}:

$$T^{EP} = \begin{bmatrix} T_{11}^{EP} & T_{12}^{EP} \\ T_{21}^{EP} & T_{22}^{EP} \end{bmatrix}. \tag{10}$$

This matrix can be assessed using a four-[5] or three-[9] microphone technique, both using two different impedance tube terminations. In the case of a homogeneous and symmetric EP, the reflection coefficient of the EP backed by an infinite air layer r_{EP} and the transmission loss coefficient TL_{EP} are given by, respectively:

$$r_{EP} = \frac{T_{11}^{EP} + \frac{1}{Z_0} T_{12}^{EP} - Z_0 T_{21}^{EP} - T_{22}^{EP}}{T_{11}^{EP} + \frac{1}{Z_0} T_{12}^{EP} + Z_0 T_{21}^{EP} + T_{22}^{EP}} \quad , \tag{11}$$

and

$$TL_{EP} = 20\log_{10}\left(\frac{1}{2} \left| T_{11}^{EP} + \frac{1}{Z_0} T_{12}^{EP} + Z_0 T_{21}^{EP} + T_{22}^{EP} \right| \right) \quad , \tag{12}$$

where Z_0 is the characteristic impedance of air.

Such measurements can be done in an impedance tube having an inner diameter of the dimension of the EP outer diameter (≈10 mm). This imposes to fabricate a tiny impedance tube with all the associated technical difficulties[3,4] (e.g., standard microphones ¼" microphones cannot be used or have to be deported, a convergent is required if a speaker larger than the tube inner diameter is used, leaks may have strong impacts…). The TMM based method proposed in this work allows using larger impedance tubes (29 mm inner diameter tubes are commonly encountered in the market). The EP is simply inserted in a rigid sample holder whose outer diameter equals the impedance tube inner diameter. A hole formed in the sample holder mimics the EC. It can be a simple cylindrical hole with a constant circular cross-section shape, or can have more realistic S-shape geometry. The surface of this perforation can be acoustically rigid or covered by a material which mimics the skin of the EC. The transfer matrix of the system "EP/sample holder" $TL_{EP,SH}$ is measured according to the procedures mentioned previously. The transfer matrix of the EP alone is then recalculated by eliminating the effect of the sample holder[10]:

$$T^{EP} = \begin{bmatrix} T_{11}^{EP,SH} & r_c T_{12}^{EP,SH} \\ T_{21}^{EP,SH} / r_c & T_{22}^{EP,SH} \end{bmatrix} \quad , \tag{13}$$

with r_c the ratio between the surface of the EP and the total surface "EP+sample holder" (equal to the surface of the impedance tube cross-section). In the case where the structure "EP+sample holder" is not symmetric, the matrix of the EP determined from Equation (13) has to be inverted first to be able to compute the reflection coefficient r_{EP} of Equation (11)[11]. The non-symmetric condition occurs for example if the EP is made of a combination of sub-layers arranged in series or if the length of the sample holder is greater than the one of the EP (see section 3).

3 FINITE ELEMENT MODELS

The proposed impedance tube experimental procedure for assessing the *IL* of the earplug is validated in this paper from numerical simulations. This section describes the chosen "EP/EC"

configuration and the numerical models based on the finite element method used to compute the *IL*.

The chosen "EP/EC" configuration is presented in Figure 2 and corresponds to the outer ear of the ATF 45CB (without the pinna) as published in ref. [12]. A silicone EP of length L=5.8 mm is inserted in an acoustically rigid and motionless EC of length l_c=24 mm. A portion of the ear canal of length l_s=10 mm is covered by a 1.7 mm-thick artificial skin layer. The rigid portion (of length 14 mm) of the ear canal corresponds to a length added by the IEC 711 coupler of the ATF. The later air cavity was modeled in ref.[12] in order to calculate power balances in the full EC. At $x=l_s$, the displacements of the artificial skin are constrained in order to mimic the ATF ear canal for which the skin layer is in direct contact with the rigid coupler. The EC ends by a locally reacting impedance Z_{TM} to account for the tympanic membrane. Both EP and artificial skin materials are modeled as elastic isotropic solids whose properties are given in Table 1. Two-dimensional (2D) finite element models of both the open and the occluded EC are solved using the software COMSOL Multiphysics (v4.4, COMSOL®, Sweden). The reader is referred to ref. [12] for a complete description of the models. Both open and occluded ear canal sound pressures averaged over the eardrum area are calculated and the *IL* is obtained from Equation (3). The *IL* obtained from the finite element models of the complete ear canal (see Figure 2) is taken as a reference and is referred to as IL_{ref} in the following.

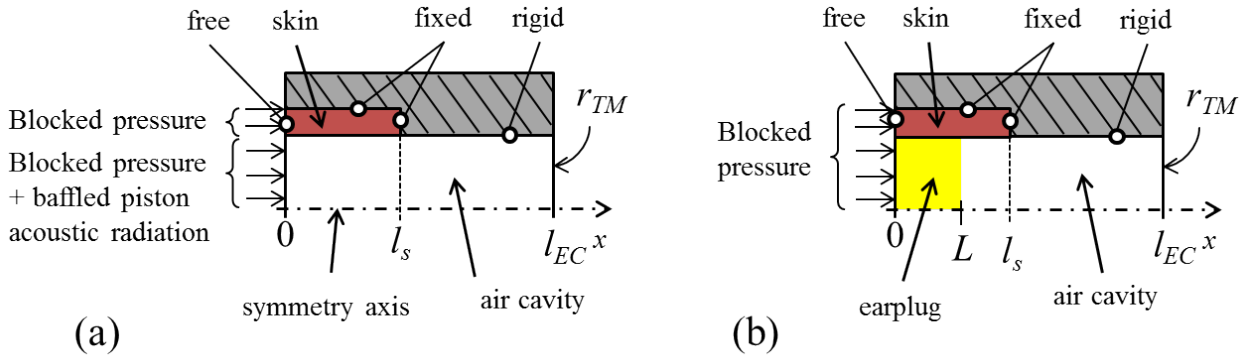

Fig. 2 – Schematic representation of the FE models of the ear canal: (a) open, (b) occluded.

Table 1 – Material properties.

Material	Earplug	Artificial skin
Young's Modulus [MPa]	1.2	0.42
Poisson's Ratio	0.48	0.43
Density [kg/m3]	1150	1050
Loss Factor	0.15	0.2

The experimental impedance tube procedure proposed in this paper is also modeled numerically. Impedance tube measurements of the "EC/EP" structure are virtually reproduced in COMSOL as shown in Figure 3. A 2D representation considering a rotational symmetry is used since the impedance tube, the EP and the sample holder are cylindrical. A unit pressure is applied on the source side to simulate the normal incidence excitation. The simulated impedance tube has an inner diameter of 29 mm. The distance between microphones 1 and 2 is 25mm. The

distance between microphone 2 and the sample is 80 mm. Finally, the two downstream cavities used for the 3-microphone technique[9] (distance between the rear face of the sample holder and the rigid backing) are respectively 30 mm and 50 mm. From the virtual measurements of the acoustic pressure at the three microphone locations (sound pressures averaged over the red area) for the two downstream cavities, the transfer matrix, normal incidence reflection coefficient and sound transmission loss of the EP alone are computed for the two configurations according to the method described previously (see Equations (11)-(13)). Finally, the *IL* is estimated by coupling the EP acoustic properties to a one-dimensional model of the occluded ear using Equations (4)-(6).

Two different configurations are investigated for which the sample holder accounts for a short or long portion of the EC as shown in Figure 3. In the first configuration (see Figure 3(a)), the transfer matrix is computed for a sample holder having the same length as the earplug. The sample holder is acoustically rigid, motionless and is covered by the artificial skin material. The two lateral faces of the skin (in contact with the air cavities) are free to move. In the second configuration (see Figure 3(b)), the transfer matrix is computed for a sample holder having the same length as the artificial skin l_s (as defined in the reference configuration of Figure 2). Furthermore, as it is the case in the ATF reference configuration, the displacements on the lateral side of the artificial skin at $x=l_s$ are constrained. Note that, for the later configuration, the EP thickness L in Equation (6) has to be replaced by the length of the sample holder (=skin length l_s) because the thin air layer between the rear face of the EP and the rear face of the sample holder is already taken into account in the simulated transfer matrix and thus on the computed TL_{EP} and r_{EP}.

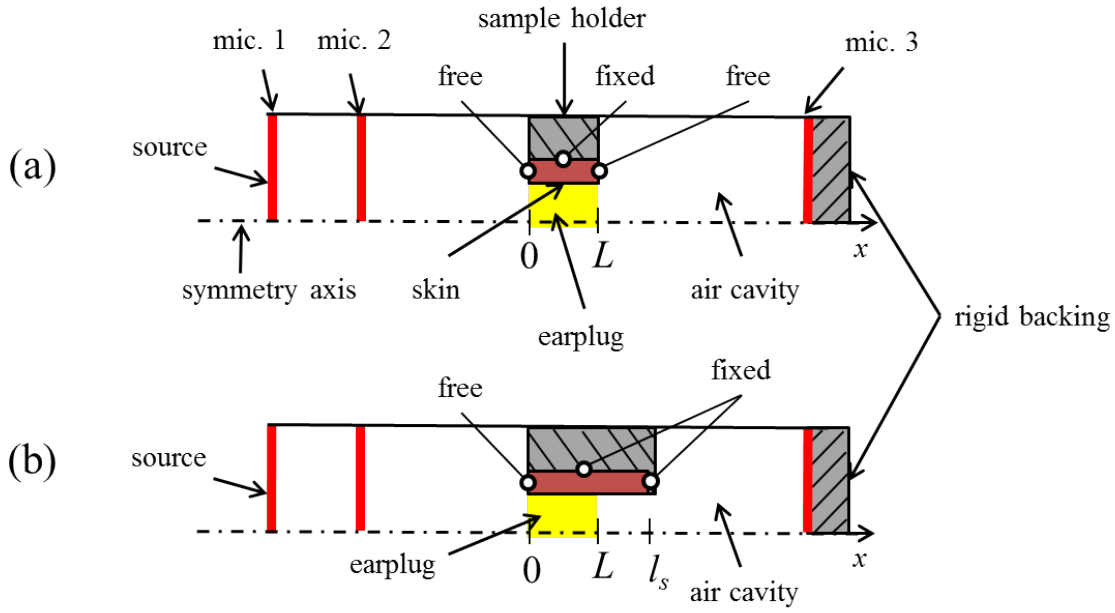

Fig. 3 – Schematic representation of the FE models of the impedance tube configurations: (a) small sample holder, (b) large sample holder with constrained skin layer.

4 RESULTS AND DISCUSSIONS

Figure 4 presents the acoustics properties of the two "EP/EC" systems of Figure 3 estimated from the virtual impedance tube measurements. The dip observed for both TL_{EP} and r_{EP} corresponds to the first EP mechanical resonance. For frequencies below this resonance, the *TL* behavior is controlled by the stiffness of the system. The *TL* of the EP inserted in the large sample holder is thus slightly superior (and the frequency of the dip shifted to higher frequencies) because the skin is constrained on one of its faces which increases the "EC/EP" equivalent stiffness.

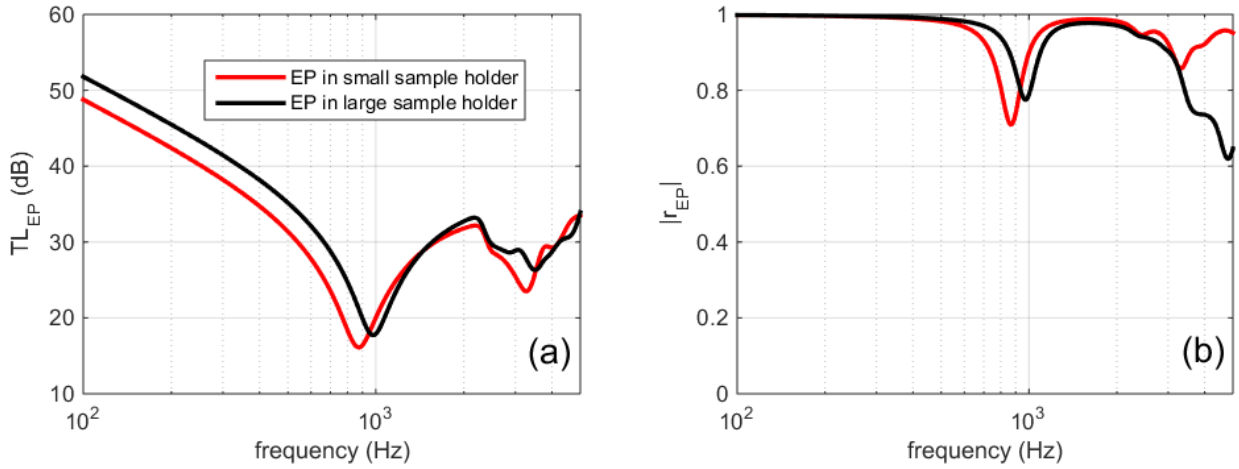

Fig. 4 – Acoustic properties of the EP computed from virtual impedance tube measurements: (a) transmission loss coefficient TL_{EP}, (b) reflection coefficient r_{EP}.

Figure 5 presents the reference *IL* computed from the finite element models of the ATF ear canal (see thick gray curve) and the two *IL* computed from the proposed impedance tube procedure based on the transfer matrix method (see red and black curves). It is shown that the *IL* obtained from the impedance tube method associated to the small sample holder (skin unconstrained at x=0 and x=L) underestimates the *IL* for frequencies up to 1 kHz. On the contrary, the *IL* estimated by the proposed method is in very good agreement with the reference *IL* in the case of the large sample holder for which the ATF skin constrain at x=l_s is accounted for. This conclusion stresses once again the great impact of the skin mechanical behavior and the coupling conditions between components (e.g., skin/bone, skin/cartilage,…) on the IL measured at low to mid frequencies.

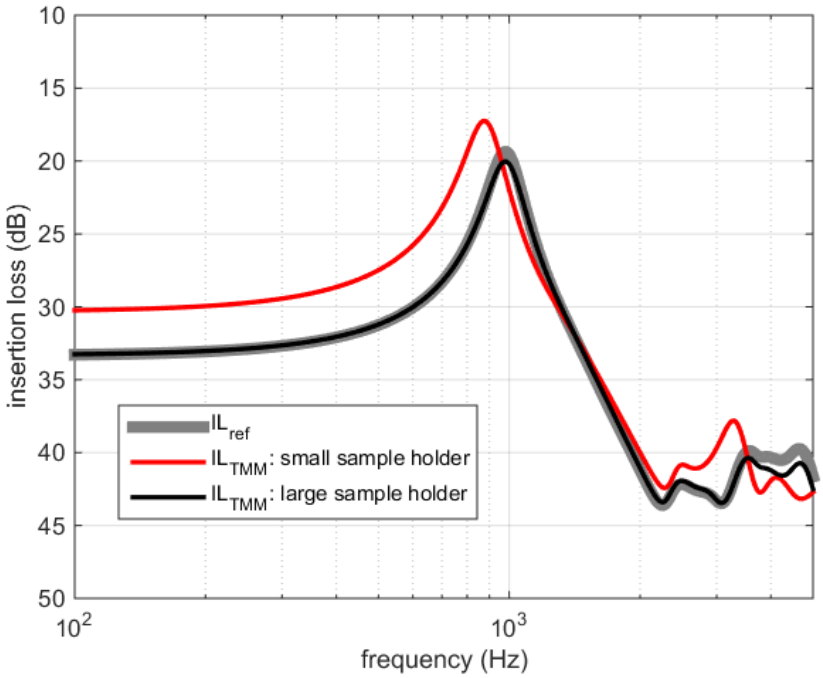

Fig. 5 – Insertion loss of the "earplug/ear canal" system.

5 CONCLUSIONS

This paper presented an experimental method for measuring the insertion loss of earplugs by the use of a classical impedance tube. This method involves impedance tube measurements of two EP acoustic properties carried out following standard procedures; the transmission loss and the reflection coefficient of the EP backed by an infinite air layer. The *IL* is then back calculated using a simple analytical expression based on several characteristic parameters of the EC/EP system such as the acoustic impedance of the tympanic membrane and the total length of the EC. The proposed method allows for measuring small EP in large diameter impedance tubes by the use of a sample holder whose inner perforation can mimic realistic EC (e.g., presence of the skin, complex geometry, human body temperature...). The validity of the proposed method was investigated numerically in the case of a silicone EP fully inserted in the ear canal of an ATF. The open and occluded ear canal of the ATF is first modeled using the finite element method and the associated *IL* is considered as a reference. The proposed impedance tube method is also tested numerically. Impedance tube measurements of the two aforementioned acoustic properties of the EP inserted in a sample holder are virtually reproduced. The *IL* is then computed using the proposed analytical relation of Eq. (4). It was shown that the proposed impedance tube method correctly predicts the ATF insertion loss of the EP provided that the sample holder mimics as much as possible the ATF skin boundary conditions. More realistic *IL*, as measured on human subjects, could thus be estimated with the proposed method if the sample holder mimics as much as possible the skin mechanical behavior and the coupling conditions between components (e.g., skin, bones, cartilage...).

6 REFERENCES

1. E.H. Burger, “Preferred methods for measuring hearing protector attenuation”, proceedings of Internoise, Rio de Janeiro, Brazil (2005).

2. D.P. Egolf, W.A. Kennedy and V.D. Larson, “Occluded-ear simulator with variable acoustic properties”, *J. Acoust. Soc. Am.*, **91**(5), 2813–2823, (1992).

3. P. Hiselius, “Method to assess acoustical two-port properties of earplugs”, *Acta Acustica united with acustica*, **90**, 137-151 (2004).

4. P. Hiselius, “Attenuation of earplugs – Objective predictions compared to subjective REAT measurements”, *Acta Acustica united with acustica*, **91**, 764-770 (2005).

5. Anonymous. Standard test method Measurement of Normal Incidence Sound Transmission of Acoustical Materials Based on the Transfer Matrix Method. American Society for Testing and Materials ASTM E2611-09.

6. G. Viallet, F. Sgard, F. Laville, and J. Boutin, “Axisymmetric versus three-dimensional finite element models for predicting the attenuation of earplugs in rigid walled ear canals,” *J. Acoust. Soc. Am.*, **134**, 4470–4480, (2013).

7. S. Maroonroge, D.C. Emanuel and T.R Letowski. *Basic anatomy of the hearing system*. In: Rash CE, et al., eds. Helmet-Mounted Displays: Sensation, Perception and Cognition Issues. Fort Rucker, Alabama: U.S. Army Aeromedical Research Laboratory, pp. 279–306 (2000).

8. J. F. Allard and N. Atalla, *Propagation of Sound in Porous Media: Modeling Sound Absorbing Materials*, 2nd ed. ,Wiley, Chichester, UK, (2009).

9. Y. Salissou, R. Panneton and O. Doutres, “Complement to standard method for measuring normal incidence sound transmission loss with three microphones,” *J. Acoust. Soc. Am.* **131**, EL216–EL222 (2012).

10. T. Dupont, P. Leclaire, K.Verdière, R. Panneton and S. Elkoun. “A method for measuring the acoustic properties of a porous sample mounted in a rigid ring in acoustic tubes”, *proceeding 21st International Congress on Acoustics* (ICA) Montreal, 2-7 June, (2013).

11. R. Panneton, “Normal incidence sound transmission loss evaluation by upstream surface impedance measurements,” *J. Acoust. Soc. Am.* **125**(3), 1490-1497 (2009).

12. G. Viallet, F. Sgard, F. Laville, and J. Boutin, “A finite element model to predict the sound attenuation of earplugs in an acoustical test fixture,” *J. Acoust. Soc. Am.*, **136**(3), 1269–1280, (2014).